

**Results on Plasma Focusing of High Energy Density  
Electron and Positron Beams**

J.S.T. Ng *et al.*

Presented at 20th International Linac Conference (Linac 2000),  
8/21/2000—8/25/2000, Monterey, CA, USA

*Stanford Linear Accelerator Center, Stanford University, Stanford, CA 94309*

---

Work supported by Department of Energy contract DE-AC03-76SF00515.

# RESULTS ON PLASMA FOCUSING OF HIGH ENERGY DENSITY ELECTRON AND POSITRON BEAMS \*

J.S.T. Ng, P. Chen, W. Craddock, F.J. Decker, R.C. Field, M.J. Hogan, R. Iverson, F. King, R.E. Kirby, T. Kotseroglou, P. Raimondi, D. Walz, SLAC, Stanford, CA. 94309, USA  
H.A. Baldis<sup>†</sup>, P. Bolton, LLNL, Livermore, CA. 94551, USA  
D. Cline, Y. Fukui, V. Kumar, UCLA, Los Angeles, CA. 90024, USA  
C. Crawford, R. Noble, FNAL, Batavia, IL. 60510, USA  
K. Nakajima, KEK, Tsukuba, Ibaraki 305-0801, Japan  
A. Ogata, Hiroshima University, Kagamiyama, Higashi-Hiroshima, 739-8526 Japan  
A.W. Weidemann, University of Tennessee, Knoxville, Tennessee 37996, USA

## Abstract

We present results from the SLAC E-150 experiment on plasma focusing of high energy density electron and, for the first time, positron beams. We also discuss measurements on plasma lens-induced synchrotron radiation, longitudinal dynamics of plasma focusing, and laser- and beam-plasma interactions.

## 1 INTRODUCTION

The plasma lens was proposed as a final focusing mechanism to achieve high luminosity for future high energy linear colliders [1]. Previous experiments to test this concept were carried out with low energy density electron beams [2]. In this paper, we present preliminary results obtained recently by the E-150 collaboration on plasma focusing of high energy density electron and positron beams.

Table 1: FFTB electron and positron beam parameters for this experiment.

| Parameter            | Value   |
|----------------------|---|
| Bunch intensity      | $1.5 \times 10^{10}$ particles per pulse                                    |
| Beam size            | 5 to 8 $\mu\text{m}$ (X),<br>3 to 5 $\mu\text{m}$ (Y)                       |
| Bunch length         | 0.7 mm  |
| Beam energy          | 29 GeV  |
| Normalized emittance | 3 to $5 \times 10^{-5}$ m-rad (X),<br>0.3 to $0.6 \times 10^{-5}$ m-rad (Y) |
| Beam density         | $\sim 7 \times 10^{16}$ $\text{cm}^{-3}$                                    |

## 2 EXPERIMENTAL SETUP

The experiment was carried out at the SLAC Final Focus Test Beam facility (FFTB)[3]. The experiment operated

\* Work supported in part by the Department of Energy under contracts DE-AC02-76CH03000, DE-AC03-76SF00515, DE-FG03-92ER40695, and DE-FG05-91ER40627, and the Univ. of California Lawrence Livermore National Laboratory, through the Institute for Laser Science and Applications, under contract No. W-7405-Eng-48; and by the US-Japan Program for Cooperation in High Energy Physics.

<sup>†</sup> Also at UC Davis, Dept. of Applied Science.

parasitically with the PEP-II B-factory; the high energy electron and positron beams were delivered to the FFTB at 1 - 10 Hz from the SLAC linac. The beam parameters are summarized in Table 1.

A layout of the beam line and a schematic drawing of the plasma chamber are shown in Figure 1. The beam size was measured using a wire scanner system. A carbon fiber 4  $\mu\text{m}$  or 7  $\mu\text{m}$  in diameter was placed downstream of the plasma lens, adjustable along the beam axis in a range of 8 to 30 mm from the center of the lens. The Bremsstrahlung photons were detected in a Cherenkov type detector located 35 m downstream of the lens. A set of ionization chambers interleaved with polyethylene blocks, located 33 m downstream of the lens, was used to monitor the synchrotron radiation emitted as a result of the strong bending of the beam particles by the plasma lens. This detector provided an independent measure of the focusing strength. Also, a Cherenkov target was installed in the electron beam line downstream to enable streak camera diagnostics of the longitudinal plasma focusing dynamics.

To create the plasma lens, a short burst (800  $\mu\text{s}$  duration) of neutral nitrogen or hydrogen gas, injected into the plasma chamber by a fast-pulsing nozzle, was ionized by a laser and/or the high energy beam. The neutral density was determined by interferometry to be  $4 \times 10^{18}$   $\text{cm}^{-3}$  for  $\text{N}_2$  and  $5 \times 10^{18}$   $\text{cm}^{-3}$  for  $\text{H}_2$  at a plenum pressure of 1000 psi. The injected gas was evacuated by a differential pumping system which made operation of the gas jet possible while maintaining ultra-high vacuum in the beam lines on either side of the chamber.

## 3 PLASMA FOCUSING

For a bunched relativistic beam traveling in vacuum, the Lorentz force induced by the collective electric and magnetic fields is nearly cancelled, making it possible to propagate over kilometers without significant increase in its emittance. In response to the intruding beam charge and current, the plasma electron distribution is re-configured to neutralize the space charge of the beam and thereby cancel its radial electric field. For a positron beam, the plasma electrons are attracted into the beam volume thus neutral-

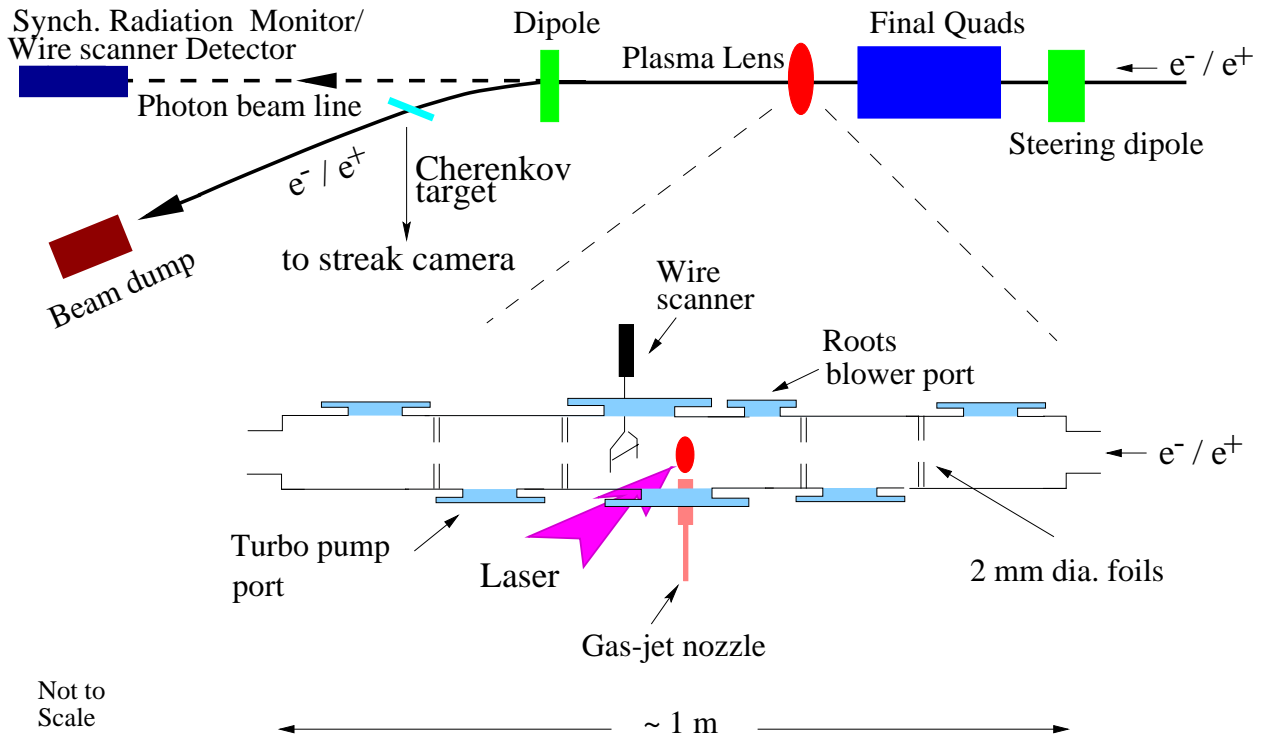


Figure 1: Layout of the plasma lens measurement setup and schematics of the plasma chamber.

izing it; for an electron beam, the plasma electrons are expelled from the beam volume, leaving behind the less mobile positive ions which neutralize the beam. When the beam radius is much smaller than the plasma wavelength, the neutralization of the intruding beam current by the plasma return current is ineffective because of the small skin depth. This leaves the azimuthal magnetic field unbalanced which then “pinches” the beam. In this experiment, typical plasma densities were of the order of  $10^{18} \text{ cm}^{-3}$ , corresponding to a plasma wavelength of approximately  $30 \mu\text{m}$  which was indeed much larger than the incoming beam radius.

The plasma was created by means of beam self-induced ionization and laser avalanche ionization. For the case of beam self-ionization, a small fraction of the neutral gas molecules was ionized due to collisions with the high energy beam particles. The secondary electrons from this impact ionization process were accelerated by the intense collective field in the beam, transverse to the direction of propagation, to further ionize the gas [4]. That is, the head of the bunch was able to ionize the gas while the core and the tail of the bunch were focused. A more quantitative understanding requires detailed calculations which are not yet available for this experimental setup.

The results on laser pre-ionization plasma focusing were obtained using a turn-key infrared ( $\lambda = 1064 \text{ nm}$ ) laser system. It delivered 1.5 Joules of energy per pulse of 10 ns FWHM at 10 Hz. The laser light was brought to a line focus at the gas jet; the plasma thus produced was approximately 0.5 mm thick as seen by the  $e^+/e^-$  beams.

With the relatively long infrared laser pulse, the pulse front was able to ionize a small fraction of the gas by multiple-photon absorption; the resulting secondary electrons were accelerated, transverse to the laser’s incident direction, to further ionize the gas. This process led to an avalanche growth in plasma density, similar to the beam self-ionization case.

### 3.1 Results on plasma focusing

The results for laser (and beam) ionization plasma focusing of electron and positron beams are shown in Figures 2 and 3, respectively. The measured transverse beam size is shown as a function of the distance ( $Z$ ) between the wire scanner and the plasma lens. The axis of the gas jet is at  $Z = -10.5 \text{ mm}$ . In the X-dimension, the beam envelope is shown converging without plasma focusing (triangle points); while with laser (and beam) induced plasma focusing (filled circles), the beam envelope is shown converging towards a reduced waist and then diverging because of the strong focusing. In the Y-dimension, the waist is at a location close to the the plasma lens beyond the reach of the wire scanner; the beam envelope is seen diverging due to the strong plasma focusing. Focusing is also observed for beam-induced plasma with the laser turned off.

## 4 OTHER RESULTS

Discussions on additional results obtained from this experiment can be found in [6]. A brief summary is given here.

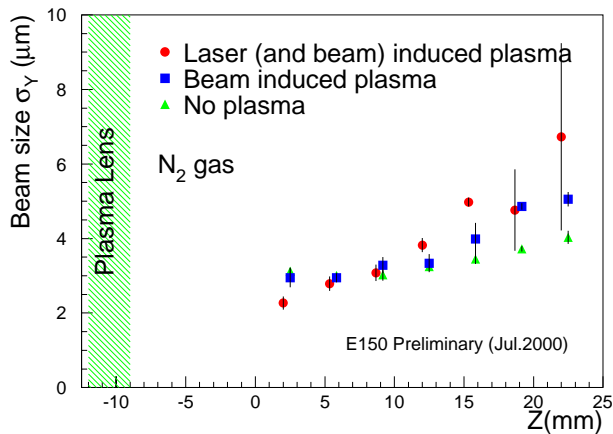
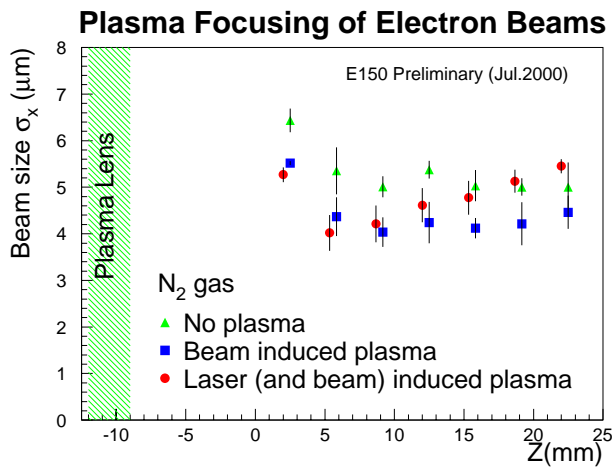


Figure 2: Plasma focusing for electron beams in the X (top) and Y (bottom) dimensions.

During the plasma focusing measurements, the focusing strength was also measured independently by monitoring the synchrotron radiation emitted by particles focused by the lens. The critical energy was estimated to be a few MeV, corresponding to a focusing gradient of  $10^6$  T/m. The longitudinal focusing dynamics was diagnosed with a streak camera with pico-second time resolution and, as expected, the focusing was strongest at the longitudinal center of the bunch. The laser- and beam-plasma interaction was studied by varying the laser pre-ionization timing with respect to the beam arrival time; we observed a delay-correlated modulation of the plasma focusing in the “after-glow” regime.

## 5 SUMMARY AND OUTLOOK

Results on plasma focusing of 29 GeV electron and, for the first time, positron beams have been presented. Beam self-ionization turned out to be an economical method for producing a plasma lens. The infrared laser with a 10 ns long pulse also proved to be efficient in plasma production, resulting in the strong focusing of electron and positron beams. Data on other aspects of plasma focusing were also collected; detailed discussion is presented elsewhere [6].

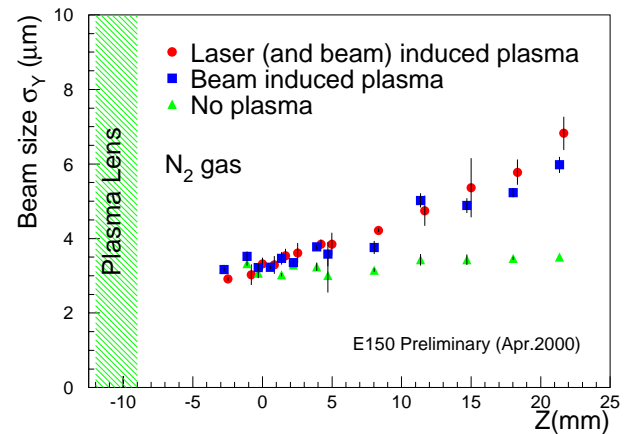
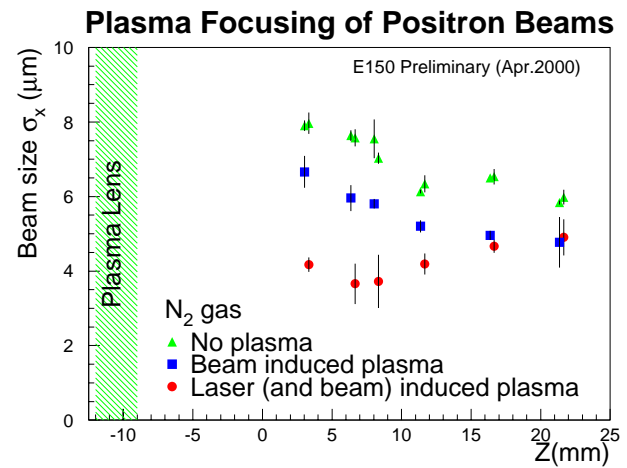


Figure 3: Plasma focusing for positron beams in the X (top) and Y (bottom) dimensions.

Design studies for linear collider applications are just starting. The first issue to resolve is the effect of beam jitter on the achievable luminosity of plasma focused beams. Optimization of plasma lens parameters requires benchmarking of computer codes as well as better understanding of the various plasma production processes. The experience gained in this experiment will serve as a basis for further engineering design studies for an eventual plasma lens application.

## 6 REFERENCES

- [1] P. Chen, *Part. Accel.*, **20**, 171(1987).
- [2] J.B. Rosenzweig *et al.*, *Phys. Fluids B* **2**, 1376(1990); H. Nakanishi *et al.*, *Phys. Rev. Lett.* **66**, 1870(1991); G. Hairapetian *et al.*, *Phys. Rev. Lett.* **72**, 2403(1994); R. Govil *et al.*, *Phys. Rev. Lett.* **83**, 3202(1999).
- [3] V. Balakin *et al.*, *Phys. Rev. Lett.* **74**, 2479(1995).
- [4] R.J. Briggs and S. Yu, LLNL Report UCID-19399, May 1982 (unpublished).
- [5] B. Chang *et al.*, *Phys. Rev. A* **47**, No. 5, 4193(1993).
- [6] J.S.T. Ng *et al.*, Proceedings of the 9th Advanced Accelerator Concepts Workshop, June 2000, Santa Fe, NM.